Ice-templated synthesis of multicomponent porous coatings via vapour sublimation and deposition polymerization

Yu-Ming Chang [a,1], Jia-Qi Xiao [a,1], Jane Christy [a,1], Chih-Yu Wu [a], Chao-Wei Huang [b], Ting-Ying Wu [a], Yu-Chih Chiang [c,d], Tzu-Hung Lin [e], Hsien-Yeh Chen [a,d,*]

[a] Department of Chemical Engineering, National Taiwan University, Taipei, 10617, Taiwan
[b] Department of Tropical Agriculture and International Cooperation, National Pingtung University of Science and Technology, Pingtung, 912301, Taiwan
[c] School of Dentistry, Graduate Institute of Clinical Dentistry, National Taiwan University and National Taiwan University Hospital, Taipei, 10048, Taiwan
[d] Molecular Imaging Center, National Taiwan University, Taipei, 10617, Taiwan
[e] Material and Chemical Research Laboratories, Industrial Technology Research Institute, Hsinchu, 31057, Taiwan

ARTICLE INFO

ABSTRACT

A multicomponent vapour-deposited porous (MVP) coating with combined physical and biochemical properties was fabricated based on a chemical vapour sublimation and deposition process. Multiple components are used based on their natural thermodynamic properties, being volatile and/or nonvolatile, resulting in the sublimation of water vapour (from an iced template), and a simultaneous deposition process of poly-*p*-xylylene occurs upon radical polymerization into a disordered structure, forming porous coatings of MVP on various substrates. In terms of physical properties, the coating technology exhibits adjustable hydrophobicity by tuning the surface morphology by timed control of the sublimation of the iced template layer from a substrate. However, by using a nonvolatile solution during fabrication, an impregnation process of the deposited poly-*p*-xylylene on such a solution with tuning contact angles produces an MVP coating with a customizable elastic modulus based on deformation-elasticity theory. Moreover, patterning physical structures with adjustable pore size and/or porosity of the coatings, as well as modulation and compartmentalization to introduce necessary boundaries of microstructures within one MVP coating layer, can be achieved during the proposed fabrication process. Finally, with a combination of defined solutions comprised of both volatile and nonvolatile multicomponents, including functional biomolecules, growth factor proteins, and living cells, the fabrication of the resultant MVP coating serves devised purposes exhibiting a variety of biological functions demonstrated with versatility for cell proliferation, osteogenesis, adipogenesis, odontogenesis, spheroid growth of stem cells, and a complex coculture system towards angiogenesis. Multicomponent porous coating technology is produced based on vapour sublimation and deposition upon radical polymerization that overturns conventional vapour-deposited coatings, resulting in only dense thin films, and in addition, the versatility of adjusting coating physical and chemical properties by exploiting the volatility mechanism of iced solution templates and accommodation of solute substances during the fabrication process. The MVP coating and the proposed fabrication technique represent a simple approach to provide a prospective interface coating layer for materials science and are attractive for unlimited applications.

1. Introduction

Surface modification by applying coatings to produce physical or chemical properties are pursued for materials to offer additional and/or multiple functions despite the natural properties of the underlying material. Physically, specifications such as surface hydrophobicity (surface energy), surface electrokinetic potential, surface roughness and topology, surface micro- and nanostructures/patterns, porosity, elasticity, mechanical strength, etc., are created [1,2]. Chemically, surface chemistry is generated by introducing functional conduct through covalent or noncovalent methods to apply chemical coatings, delivering specific and orthogonal, as well as nonspecific, reactivities and to enable additional chemical functions [3,4]. Distributions and configurations of these surface physical and chemical properties with advanced controls from a

---

conventional homogeneous layout into an advanced fashion showing anisotropic, hierarchical, and gradient configurations are attractive and are developed to fulfil more complex and prospective materials across multidisciplinary material science fields [5,6].

The aforementioned surface properties are particularly important and sophisticated for biomaterials science, with more stringent requirements due to complexity in the microenvironments of a variety of biointerface properties encountered [7,8]. For instance, cells can respond to environmental cues and result in intercellular and intracellular changes in cytoskeletal organization, proliferation, cell differentiation, gene expression, and apoptosis [9,10]. Modifications of physical properties with generated porous structures include: elasticity [11,12], topology [13,14], surface roughness [15], 2-D and 3-D surface structures [16], and geometrical changes [17]. The cascades of these physical sensing procedures are also fundamental in cell biology, tissue engineering, and medicine [18]. Chemical coatings have demonstrated modified long-term performance and efficiency for biodevices and biomaterials by a wide spectrum of bioorthogonal reactions [19], providing reaction rapidity and specificity in manipulating proteins [20], glycans [21], synthetic molecules, e.g., fluorescent dyes [22], polyethylene glycol [23] and modifications to mimic cell extracellular matrix (ECM) ligands [24] for the performance and tolerance of biomaterials towards a diversified array of other functionalities in their native environment or in the complexity of a living cell [19]. A coating with combined physical and chemical complexities and properties has been developed but with limited fabrication approaches and problematic processing conditions [25]. Existing methods of generating structural coatings by using porogenic substances followed by crosslinking the coating network have been reported [26], or composite coatings can also be created by electrochemical and electrophoretic deposition [27], defined structures and patterns can be produced by interventional processes including templating [28], photolithography [29], soft lithography [30], and by additive approaches including 3D printing [31], laser sintering, projection stereolithography [32], electrified jetting [33], spray coating [34], the weaving technique [35], or direct writing [36], which are used to build up such porous coating materials in a layer-by-layer or stacking manner. Chemical functionalization of the coatings was, however, introduced during the process or by postmodification and mostly demanded substantial knowledge to perform chemical reactions under harsh conditions [37]. Collectively, existing challenges are limited by the large number of processing steps required, efforts of removing the template [30], poor control and low efficiency of the production parameters, and sophistication of computer programming [31] and/or manual intervention [35] to perform 3D-printed coatings, and finally, the fact that these methods are limited in solution-based operation conditions. The well-known vapour deposition approaches to prepare coatings have thus far been described to create only dense films and coatings on a substrate [38], and the formation of surface structures, e.g., porous structures and patterns, is formulated in a postmodification fashion [39].

In the present study, we show that a multifunctional vapour-deposited porous (MVP) coating is fabricated on material substrates rather than a layered dense film based on vapour-phase polymerization and construction from an iced template in one step. Acknowledging that a well-established vapour deposition coating material of poly-*p*-xylylene is deposited with a conventional adsorption limited mechanism [40] forming a dense thin coating film, we recently discovered and overturned the deposition with a diffusion-limited mechanism [41,42], in which the deposition occurs on a mobile surface of a sublimating template (vapour sublimation) instead of a stationary substrate. The overall process allows the deposition and polymerization of poly-*p*-xylylene in the third depth dimension and with the formation of pore structures. We additionally hypothesize that the vapour sublimation and vapour deposition process is used to prepare a porous coating of MVP on a range of substrate materials and that the rationale functionalization to exhibit physical and/or biochemical functions for such an MVP coating is created by the manipulation and control of mass transport to accommodate additive

molecules that either participate or are excluded from the proposed vapour sublimation and vapour deposition mechanism, and decorations of these additive molecules are performed in multiple cascades and in a defined composition and spatial configuration (Fig. 1a). The final construction of the MVP coating exhibited the advised multiple functions with versatility of selecting additive molecules (e.g., biomolecules, macromolecules, proteins, drug molecules, nano-to submicron particles, living cells, etc.) for the users. Compared to existing methods of coating fabrication, the introduced MVP coatings provide advantages: (i) simple steps and vapour-base fabrication processes are used, avoiding complex procedures and harsh solutions, potentially offering preservation of sensitive molecules, (ii) use mass transport control involving vapour sublimation of volatile additive molecules during fabrication is used to exhibit adjustability of pore structures and mechanical strengths, (iii) controlled freezing procedures are used during the same fabrication process to provide adjustability of the coating morphology and the resultant surface hydrophobicity, (iv) nonvolatile liquids are used during the fabrication process with modifications of the liquid/coating compositions and structures to render customizable surface elasticity, (v) spatial arrangement and compartmentalization of the iced template are used to create structured MVP coatings and with compartmentalized biochemical boundaries within the coating structure, and (vi) the same versatile accommodation procedure used in (ii) and (iv) during fabrication are used to introduce multiple functional additives including biomolecules, growth factor proteins, and even living cells to multiply the chemical and functionalization of the MVP procedure in varying coatings. The proposed coating technology represents a prospective coating layer for the modification of material surfaces, provides a multiplied combination of physical and biochemical modification functions that are customizable to meet the increasing complexity of biological microenvironments and is fabricated based on a state-of-the-art, vapour-based sublimation and deposition polymerization process in simple steps, exhibiting breakthroughs in coating technology that are still limited by current solution-based coating technologies.

2. Results and discussion

In light of the vapour-phased, adsorption-limited polymerization of poly-*p*-xylylenes, of which the quinodimethane monomers were deposited on a mobile and sublimating surface, e.g., a sublimating iced, dry ice, etc. [42], and the quinodimethanes polymerized upon nucleation into a disordered poly-*p*-xylylene polymer structure in three dimensions, and pores were formed during the escaped water vapour and due to the voidage by the polymer structure [41], a preparation of an ice template on theoretically any substrate materials was thus exploited with such a vapour sublimation and deposition process to produce porous coatings of poly-p-xylenes (MVP coatings). In the experiments, intuitively, ice templates were prepared as a base and sacrificed coating on substrate/surfaces by first adsorbing water molecules by methods such as immersion in water solution, spraying of water vapour, water condensation at reduced temperature, etc. [43], and such a base coating of iced film/template thus formed by a solidification process with gradually reducing the temperature or instantly under liquid nitrogen conditions [44]. Subsequently, with the proposed vapour sublimation and vapour deposition under devised thermodynamic conditions of reduced pressure at approximately 0.1 bar and 20 °C, a porous coating of poly-*p*-xylylene formed by causing the iced template to vanish and creating a porous poly-*p*-xylylene layer on the same substrate surface. During the vapour construction of the MVP coating, an analysis using a real-time mass spectrometric gas analyser verified a characteristic peak of the sublimated water molecules at 18 amu and peaks for the deposited *p*-quinodimethanes and derivatives at 104 amu and 139 amu, revealing evidence of poly-*p*-xylylene deposition (Fig. 1b). Structural characterization of the resultant MVP coating was further performed by using a combination of laser confocal microscopy and microcomputed tomography (micro-CT). The laser confocal image showed a homogeneous porous structure for the
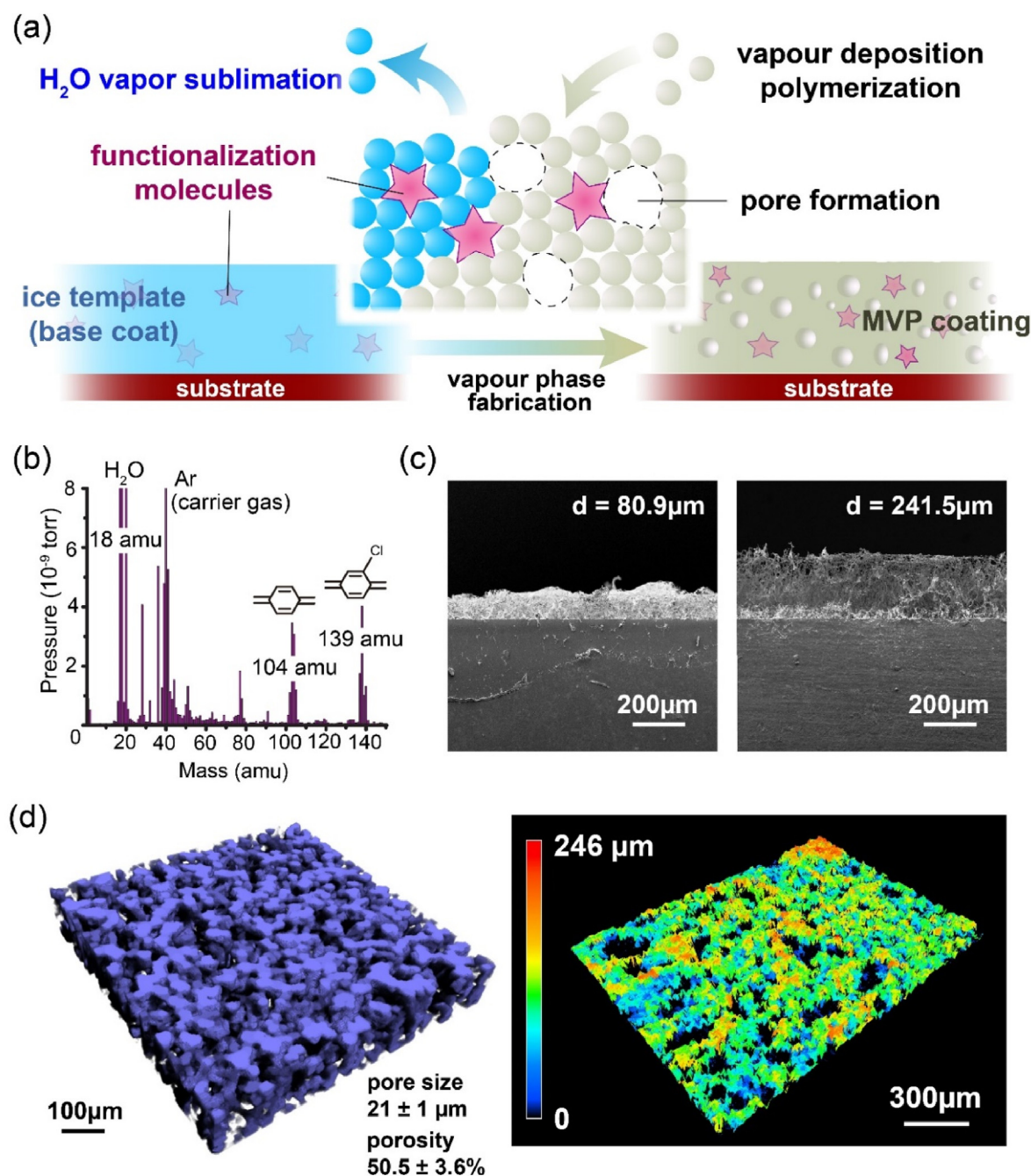
Fig. 1. (a) Schematic illustration of the fabrication process of the MVP coating on a substrate based on the vapour sublimation and vapour deposition mechanism and process. Defined physical and/or biochemical properties of the MVP coating are modified and decorated based on impregnation of additive molecules during the vapour-phase process. Controlling the composition and spatial configuration of the additive molecules was performed and selected with their volatile and nonvolatile nature to participate in the vapour sublimation stage. (b) Analysis by real-time mass spectrometry during the fabrication process indicative of the presence of water molecules (sublimating vapour) at 18 amu and quinodimethane monomers (depositing vapour) at 104 and 139 amu. (c) The SEM images showed the resultant MVP coatings with cross-sectional viewpoint of selected thickness of approximately 80.9 μm and 241.5 μm were fabricated. (d) The 3-D profile and micro-CT analysis showed a computed and reconstructed 3-D porous structure image; the calculated pore size distribution was approximately 21 ± 1.0 μm, and the degree of porosity was approximately $50.5 \pm 3.6\%$.

coating with a measured average pore size of approximately 23.9 ± 5.6 μm. Images recorded by micro-CT showed three-dimensional structures of the coating. Interconnected pores were observed with a measured porosity of approximately $50.5 \pm 3.6\%$, and 99.9% connectivity was estimated by the micro-CT computing software. The calculations from the micro-CT data indicated an approximately 21 ± 1 μm pore size distribution, which unambiguously supported the consistency of the results by laser confocal microscopy. With acknowledgement that varied

thicknesses of prepared iced templates can be formed with limited controllability, the final thickness of the MVP coating, on the contrary, was controlled by a stagewise sublimation and deposition process to obtain a desired thickness [41,45], in which time-controlled sublimation was performed by stripping the ice template of shrinkage volume and perimeter to a desirable thickness and subsequently introducing the deposition of poly-*p*-xylylene to finalize the MVP coating thickness. As indicated in Fig. 1c, a thickness of approximately 241.5 μm of MVP
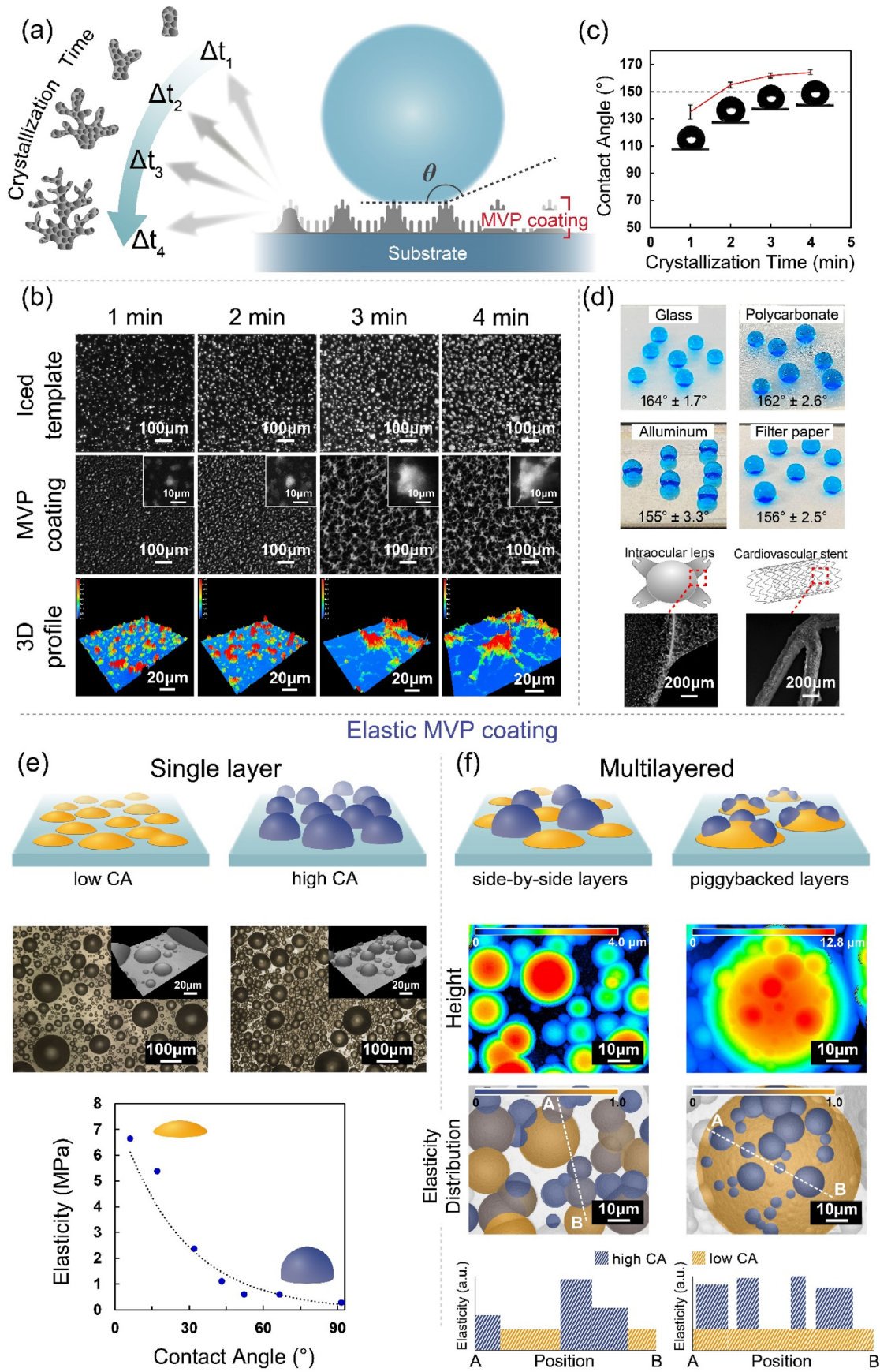
(caption on next page)

Fig. 2. (a) A time-controlled frost/ice template with anisotropic structures was prepared by rapid cooling conditions with respect to time, and replicated structures with the same anisotropy of the surface structure of an MVP coating were formed during the vapour-phase fabrication process, providing increasing super-hydrophobicity according to the processing time. (b) Optical micrographs indicated increasing complexity of the anisotropic structure of the prepared frost/ice template with respect to the cooling processing time, and after the vapour-phase process to construct the MVP coatings, the images showed consistency of increasing complexity of surface structures. The 3-D profile images also confirmed these anisotropic structures of these time-controlled fabricated MVP coatings in three dimensions. (c) A tendency of increasing the surface superhydrophobicity (water contact angle) was analysed proportional to the processing time and due to the increasing complexity of the constructed surface structures. (d) The superhydrophobic MVP coatings could be prepared by the proposed fabrication process on a variety of substrate materials, including glass, a polycarbonate polymer, aluminium metal, and cellulose filter paper, as well as on complex substrates of a vascular stent and a curved surface on an intraocular lens. Water droplets were stained with blue dye to guide vision. (e) An illustration shows the fabrication of an MVP coating with controllable elasticity based on using tempered and nonsublimated liquids as ice/liquid templates during the vapour-phase process. The optical micrographs and the 3D profile images showed that the liquids were prepared with varied contact angles to fabricate the MVP coatings. A statistical analysis revealed correlations between varied contact angles and elasticity. (f) Fabrication of the MVP coating with multiple layers of liquid templates, producing spatially configured elasticity in two dimensions and in three dimensions. A simulated and calculated elasticity vs. spatial position was shown with an overlapped bright field image to predict the multiple stages and distributions of elasticity in 2D and 3D. (For interpretation of the references to colour/colour in this figure legend, the reader is referred to the Web version of this article.)

coating was obtained by concurrent sublimation and deposition without time control, while a devised 80.9 μm thickness of MVP coating was achieved by 360 s of stagewise control of sublimation and deposition.

For the sake of generating and controlling physical and structural coatings of MVP, the offering of adjusting surface (super)hydrophobicity was first demonstrated by a timed control of crystalline and roughened structure when preparing the iced templates, and the proposed sublimation and deposition process rendered an MVP coating with the same time-controlled surface structures and customized surface hydrophobicity (Fig. 2a). During the experiment, the iced templates were prepared first by a condensation process forming a layer of ice frost on a chosen substrate of a glass with instant reduction of temperature to approximately −50 °C (by a liquid nitrogen bath) on such a substrate. The condensation enabled a phase transition of ambient water from a vapour phase to a solid-state ice frost, with skipping the liquid phase due to an instant temperature difference between the substrate surface and its ambient environment [46], and anisotropic granules of ice frost crystals were discovered in the prepared iced template on glass substrates (Fig. 2b). Compared to a gradual condensation process with an existing dew point and liquid-phased water, a smoothed water-air interface [47] forming the same smooth homogeneous surface structure is the result for the iced templates. These data are included in the Supporting Information in Fig. S1a. The surface hydrophobicity was measured with an average 135.1° ± 5.3° water contact angle due to the created anisotropic structures as well as the hierarchical surface roughness (shown in Fig. S1c) that is crucial to the surface hydrophobicity based on the Cassie-Baxter theory [48]. In addition, a timed dependence of controlling the formation and crystallization indicating an increasing grain size and structure density was found for fabricating the anisotropic structures on the iced templates and the same produced MVP coatings. An increase in superhydrophobicity was also found to be dependent on timed structural control of the MVP coating, and the water contact angles of the resultant coating surfaces were measured from 135.1° ± 5.3°, 157.3° ± 2.1°, 161.9° ± 1.9°, to 164.4° ± 1.7° according to the controlled crystalline time frames of 1, 2, 3 and 4 min, respectively, as indicated in Fig. 2c. The contact angle hysteresis of the resultant coating surfaces were also measured according to a reported method [49]. For the coating surfaces of crystalline time of 4 min, the corresponding contact angle hysteresis was measured with an average of 8.3° ± 0.7°, while the results of coating surfaces of crystalline time below 4 min were found to be unmeasurable due to the droplets sticking on the coating surfaces, which was believed to be due to the transition from the Cassie–Baxter state to the Wenzel state as the surface roughness decreases with decreasing crystalline time frames [50]. The wide applicability to prepare such structural MVP coatings with administered superhydrophobicity for a variety of substrate materials was also demonstrated on selected substrates, including zirconium dioxide ceramic, polycarbonate plastic, aluminium metal, and cellulose paper; consistent results of averaged water contact angles between 155° and 164° were found for applying the MVP coatings on these substrates. Furthermore, the applicability of these MVP coatings on

curved surfaces and complex devices, e.g., an intraocular lens and a cardiovascular stent, was also demonstrated in a facility, as shown in Fig. 2d.

The fabrication of the structural MVP coating was further extended to enable a coated substrate surface to have controllable elasticity. Acknowledging that exploiting a nonvolatile solution during the vapour sublimation and deposition process can result in only the vapour deposition and encapsulation of poly-*p*-xylylene on the nonsublimated solution surface, and a promised coating fidelity over topologies can form conformal coatings on the cultures of the liquids [51], we thus proposed the fabrication of an MVP coating by using tempered liquids (by engineering surface contact angles of the underlying surfaces and/or the liquids) [51] for the vapour fabrication of MVP coatings. The encapsulation upon deposition of modified hydrophobicity of droplets with varied shapes to render coatings exhibiting customizable elastic modulus based on deformation-elasticity theory [52,53], as well as a layered display of encapsulating multiple liquids with varied hydrophobicity, i.e., the resultant coating surfaces contained side-by-side, varied and controlled elastic properties and provided multiplied access channels to controlled and varied elasticity properties. During fabrication, the preparation of the ice template was now a permanent liquid layer rather than a sacrifice and sublimation template, and the liquid layer was prepared to sustain a satisfactory contact angle based on the concept discussed in the previous section or other similar liquid/surface energy balance theories [54]. Intuitively, a selection of a nonvolatile liquid material, e.g., polyethylene glycol and glycerol oil, and/or a control of surface hydrophobicity, e.g., plasma and silanization, are commonly used to control the liquid/surface hydrophobicity behaviours and are well documented [55]. A solidification process of reducing the substrate temperature for the preparation of the liquid templates was trivial during fabrication, and the temperature difference only resulted in the deposition thickness of the outer coating layers of poly-*p*-xylylenes [56]. As indicated in the 3-D profile images in Fig. 2e, liquid layers with varied surface hydrophobicities were first prepared on hydrophobic-modified glass substrates and showed administered contact angles (CAs) in a wide range from 6.5° ± 0.8°–93.5° ± 2.7°. Subsequently, the vapour deposition of poly-*p*-xylylene on such liquid templates resulted in the fabrication of MVP coatings with the proposed and varied elasticity properties. Characterization method of elastic modulus of fabricated MVP coatings were described in Fig. S2, and the corresponding elastic modulus ranging from 0.288 MPa to 6.66 MPa, with correlation to varying CA of liquid layer of the MVP coating, are shown in Fig. 2e. An anticipated tendency of predictability for future design of a coating elastic property confirmed that a lower elastic modulus for increasing CA exhibiting consistency to the deformation-elasticity theory was discovered for such fabricated MVP coatings. Furthermore, in addition to the single layer liquid template, the fabrication of multiple layers of liquid templates with an arrangement of distinct CAs for these layers of liquids was performed to create an elastic MVP coating with spatially controlled elasticity in two dimensions and/or three dimensions. An equilibrium to

separate the configuration of low CA and high CA liquid layers was discovered to be homogeneous and side-by-side in two spatial dimensions in the fabrication of the multilayered coatings and was believed to be due to a favoured thermodynamic surface energy with a small sliding angle (disfavoured affinity) between the low CA liquid and a hydrophobic surface [56] (experimental data are also included in the Supporting Information in Fig. S1b. In contrast, hydrophobic affinity between a high CA liquid and a hydrophobic surface was found to produce a piggyback-like configuration of a multilayered MVP coating that comprised a two-stagewise elasticity in the third dimension (z-direction). As indicated in Fig. 2f, the 3D topographical profile images revealed the two configurations of the controlled and multitude elastic MVP coatings, and a spatial elasticity map was calculated and constructed based on the mapping of liquid droplet of which size and height determine the CA value and corresponding elasticity moduli. With respect to the overlapped droplets in the piggyback-like configuration, the overall elasticity was calculated based on the "rule of mixtures" among which the Reuss isostress assumption was adopted [57]. Designable parameters can theoretically be engineered to predict a desirable surface elasticity in 2D and 3D for prospective MVP coating fabrication.

However, the fundamental importance of the MVP coatings to provide topological and structural controls enabled possibilities for applications such as analytical/diagnostic devices, DNA, protein, cell arrays, micro-/nanofluidic systems that require coatings with structural capability and features. In the demonstration, an intuitive approach using polydimethylsiloxane (PDMS) moulding and forming arrayed ice templates with dimensions of 300 μm × 300 μm x 300 μm was used for the vapour sublimation and deposition process to fabricate the proposed structural MVP coatings. Theoretically, other methods of creating iced templates can also be prepared by softlithography [58], sculpturing [59], directional freezing and crystallinity [60], and direct assembly and modulation [61].

As indicated in Fig. 3a, the moulded ice templates on the substrate surfaces were subjected to the proposed vapour sublimation and deposition fabrication process and the described mechanism, forming an MVP coating with fairly replicated structures of the templates, i.e., a structured/patterned coating comprised of poly-*p*-xylylene polymer with an outlook architecture of 300 μm × 300 μm x 300 μm arrays and porous interior structures. A rationale for controlling the pore size and the porosity for these structured MVP coatings was further performed based on a previously reported mechanism in which the sublimation rate (sublimated volume) of the ice template is proportional to the control of the processing temperature and/or the thermodynamic sublimation nature of a selected material to prepare such an iced template, e.g., hexane, ethanol, acetone [41], and theoretically, defined mixtures with varied sublimation properties of the materials were used to fabricate controlled distributions of pore size and porosity in gradient or hierarchical fashion [62]. A showcase, therefore, in Fig. 3a, indicated fabricated and patterned MVP coatings with pore sizes controlled from 1.4 ± 0.5 μm, 4.7 ± 0.7 μm, 16.2 ± 2.7 μm, to 70.4 ± 12.9 μm based on varying the sublimation temperatures from $-4\,°C$, $5\,°C$, $15\,°C$, to $35\,°C$, respectively, while using the agreed water solution as a single component system to prepare the iced templates and for deposition and fabrication.

Finally, in the fabrication of structural MVP coatings, complex structures with defined compartments and configurations with a discrete boundary between different compartments were established in one patterned structure by the same one-step continuous vapour sublimation and deposition process regardless of a discontinued assembly of prepared ice templates, i.e., the volatile water molecules vanished in the sublimation stage, and the nonvolatile components (solutes) were preserved in a preset spatial location and composition in the advised compartments.

Preparation of the ice templates was facilitated analogously to a multicomponent ice bar made during sequenced moulding and cooling procedures (two moulding and two cooling procedures were performed in the current study). In the demonstration in Fig. 3b, combinations of two solution systems with defined and varied solution composition were prepared for moulding in sequence with varied shapes and cooling procedures, forming the proposed iced templates/base coats that were composed of physically complex and separate boundaries and compartments, and chemically, varied compositions were configured in the devised and separated compartments of the structured ice template/base coats. Subsequently, these substrate samples with such complex ice base coats were then used for the same vapour deposition process to result in the final MVP coatings with decorated interior physical compartments and modified chemical compositions. As indicated in Fig. 3c, the fabricated MVP coating layers exhibited the same complex multicomponent and compartments in defined structures and compositions, and examples showed sharp boundaries separating distinct fluorescent molecules of Oil Red O (red channel) and fluorescein-5-isothiocyanite (green channel) in the corresponding compartments that were programmed by the same configurations of prepared complex ice templates. Furthermore, the creation of an MVP coating to enable even more complicated biological microenvironments and boundaries in one structured coating layer was performed using such a compartmentalization concept, i.e., a more sophisticated coating layer to contain a first combination of biomolecules and living cells in the first structured compartment and a second combination of biomolecules and cells in the second compartment. As shown in Fig. 3d, cell-laden MVP coatings were constructed and structured to separate 3T3 fibroblasts with the fibroblast growth factor (FGF-2) concept in the first compartment (green channel) and human osteoblasts (MG-63) along with bone morphogenetic proteins (BMP-2) in the second compartment. The laser confocal images also confirmed these structured compartments in three dimensions of the fabricated MVP coating. Notably, an oil-in-water system was exploited for preparing cells in the iced templates to exclude vapour sublimation and to avoid frostbite during the cooling procedures [63] and to sustain viable cells [64] in the final MVP coating constructs. The results collectively showed that the proposed structuring and patterning of MVP coatings was realized from conventional top-down surface structuring to the creation of a more sophisticated and multicomponent interior structure with compartmentalization, and the necessary boundaries were established and constructed in one coating layer of MVP with versatility to fulfil design requirements in dimension, shape, porosity, and biochemical compositions.

Finally, in the fabrication of MVP coatings of biochemical functionalization, an elegant control of exploiting a multicomponent solution comprised of volatile solvent (water) and nonvolatile additives (functional biomolecules, cells, etc.) was performed to prepare the ice templates, and the same vapour sublimation and deposition fabrication process finally rendered an MVP coating performing desired biological functions in time and in cascades based on the nonvolatile additives towards its surrounding microenvironments. A schematic image showing the concept of the biochemical functionalization is shown in Fig. 4a. During the fabrication process, the nonvolatile additives remain in the fabrication chamber, while water was sublimated, and a negligible loss of the nonvolatile additives was observed. With the same concept, various coatings could be fabricated to perform desired functions based on the added functional additives, which would adsorb to the fabricated coatings. Examinations of the biocompatibility and cell viability of such fabricated MVP coatings were analysed. Based on an MTT (3-(4,5-dimethylthiazol-2-yl)-2,5-diphenyltetrazolium bromide) assay, an overall >95% and >85% viability (1 or 3 days) was discovered for the 3T3 cells cultured on the MVP coatings and on the samples in which the cells were accommodated within the MVP coating layers, respectively. The experiments were also performed in parallel on tissue culture polystyrene (TCPS) plates as the control group for the comparisons, and the statistical analysis showed the proliferation ratios of the cultured 3T3 cells exhibited consistency and high biocompatibility for all the samples including 3T3 cells on top on MVP and 3T3 cell-laden MVP, and the data revealed no significant difference in comparison to the TCPS control group. These data are included in the Supporting Information in Fig. S3.

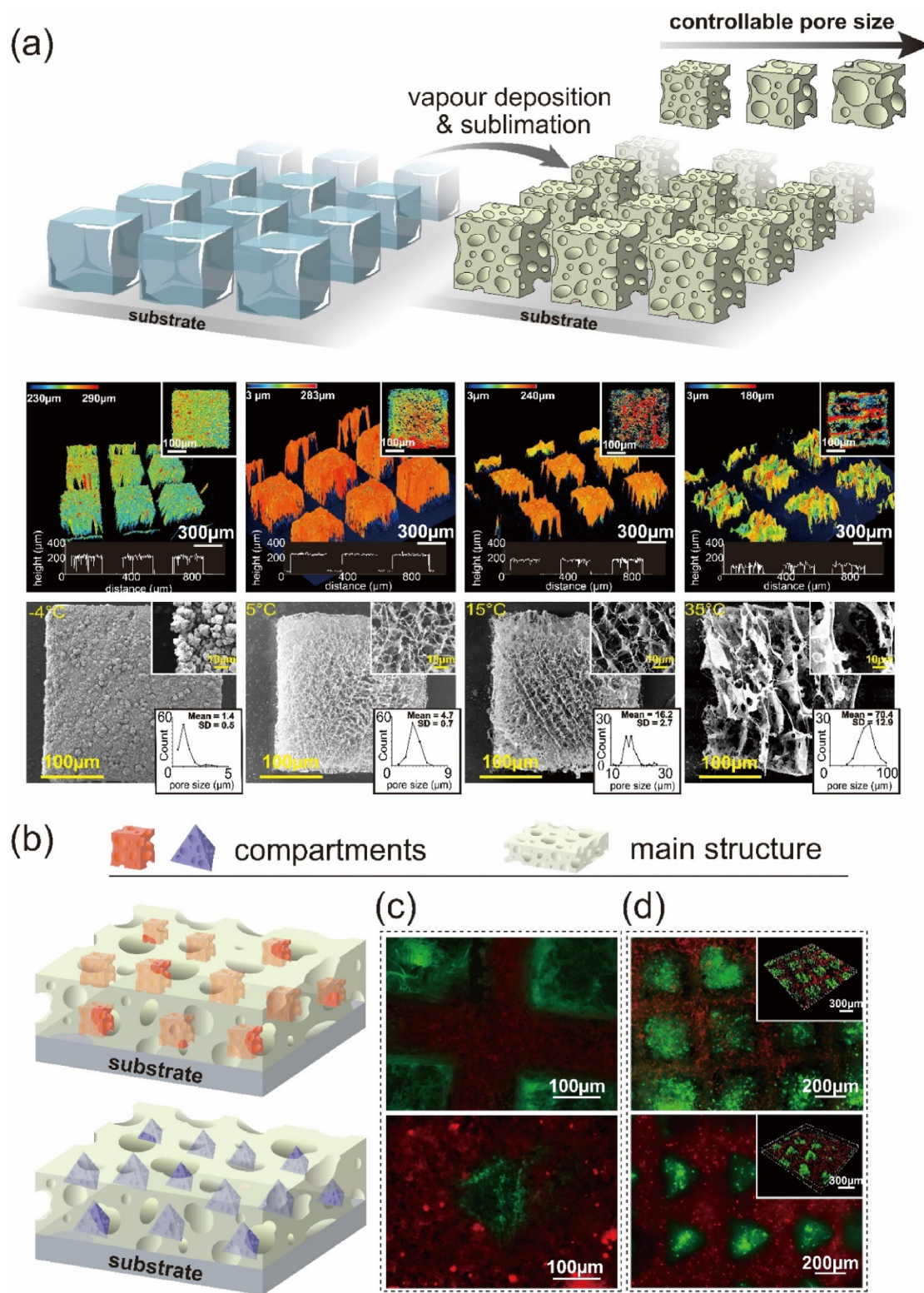The important biochemical functionality modification of the

Fig. 3. (a) An illustration showing the fabrication of a structural MVP coating from the moulded ice template. 3-D profile images and SEM micrographs showed the same 300 μm × 300 μm x 300 μm MVP coating outer dimensions but with varied pore size controllability by the proposed fabrication process. Detailed and enlarged fields of view and the cross-sectional profiles are shown in the insets. (b) A complex structural MVP coating with defined compartments and configurations with a discrete boundary between different compartments was established by the fabrication process. (c) Fluorescence and laser confocal micrographs showed structured compartments comprised of Oil Red O (red channel) and fluorescein-5-isothiocyanite (green channel) for the fabricated MVP coatings with different shapes and dimensions. (d) Versatility of using the fabrication technology to construct a complex and structural MVP coating with delicate compartments and boundaries to separate 3T3 fibroblasts with fibroblast growth factors (FGF-2) in the first compartment (green channel) and human osteoblasts (MG-63) along with bone morphogenetic proteins (BMP-2) in the second compartment was also demonstrated. (For interpretation of the references to colour/colour in this figure legend, the reader is referred to the Web version of this article.)
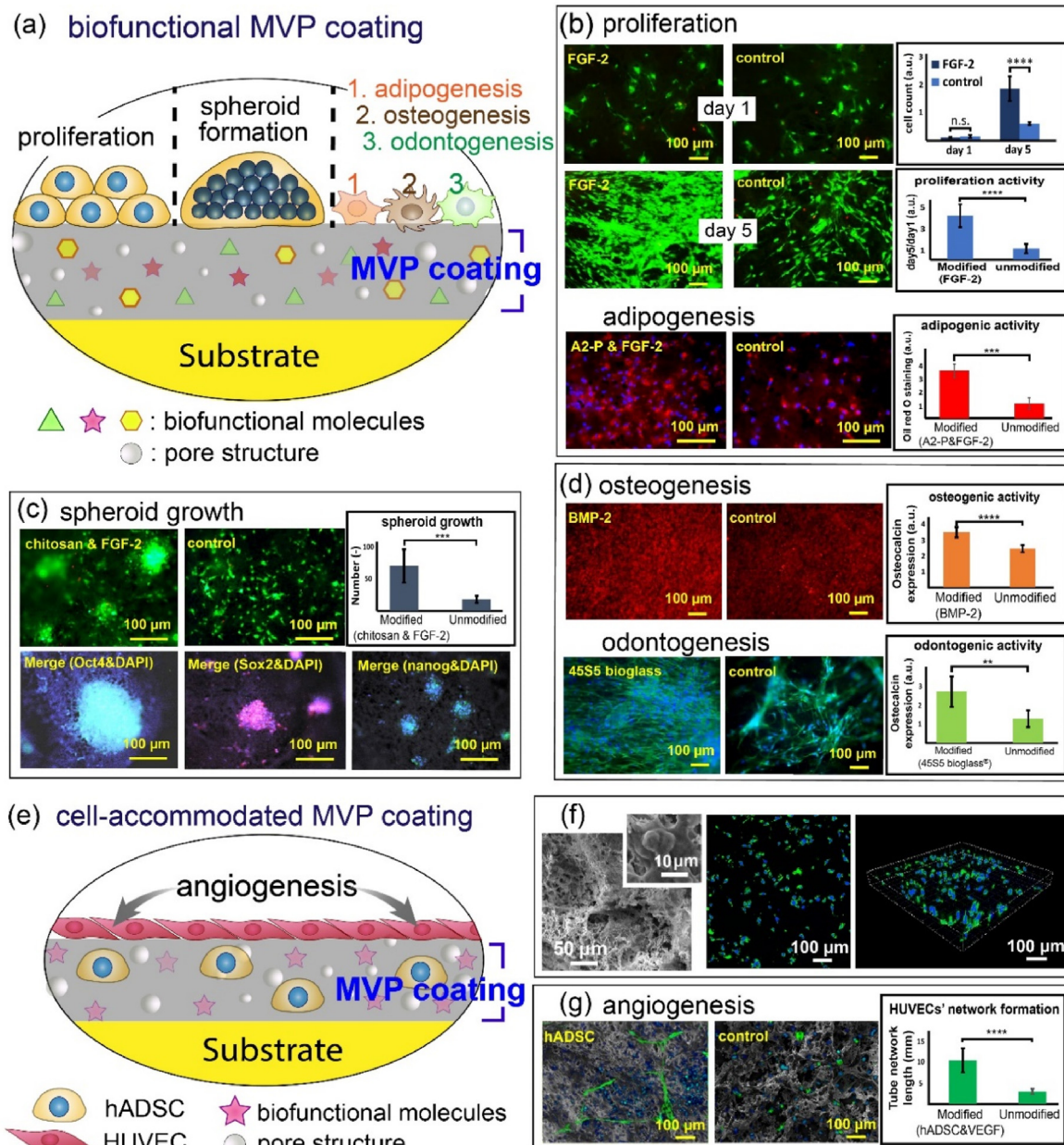
Fig. 4. (a) An illustration showing the biological functionalization of the MVP coating based on impregnation of a multicomponent solution comprised of volatile solvent (water), nonvolatile additives (functional biomolecules, living cells, etc.) to prepare ice templates, and the proposed vapour sublimation and deposition mechanism resulted in the final fabrication of biochemically functionalized MVP coatings. (b) A combination of FGF-2 and A2-P impregnation for the MVP coating was used to demonstrate the maintained stemness and proliferation of hADSCs cultured on the MVP coating compared on Day 1 and Day 5 and was shown to significantly enhance the cell population and upregulate stemness. A verification showed straightforward and guided adipogenic differentiation with the same expected enhancement, as shown by staining with Oil Red O and statistical analysis. (c) A second combination of FGF-2 and chitosan impregnation and modification for the fabrication of the MVP coating enabled the formation of hADSC spheroids. Upregulated expression of the stem cell pluripotent markers Oct4, Sox2, and nanog statistically confirmed the enhancement of hADSC spheroids by this combination in MVP coating. (d) Versatility of varying the combination of functional substances including BMP-2 and/or 45S5 Bioglass® during the impregnation and fabrication of MVP coatings for enhancements of bone morphology related differentiations of osteogenesis from hADSCs and odontogenesis from hDPSCs were demonstrated by showing upregulated cellular morphology and the expression of osteocalcin. (e) A state-of-the-art combination and modification to fabricate an MVP coating comprised of impregnated living cells of hADSCs and VEGF molecules was demonstrated with coculture and for the enhancement and promotion of HUVEC growth and maturation activities. (f) SEM and fluorescence micrographs (2D and 3D) showed accommodation of living hADSCs cells within the MVP coating layer. Overlaying fluorescence channel was performed in the micrographs by showing F-actin cyto-skeleton in green channel and cell nucleus in blue channel. (g) Luminal tube network formation of cultured HUVECs, indictive of angiogenesis activity on the MVP coating comprised of accommodated living hADSCs and VEGF at day 10. CD 31 markers of HUVEC were stained in green channel, and the nuclei of hADSCs were stained in the blue channel. Statistical analysis was performed by measuring the length of tubular network and the data were compared to a pure MVP coating without modification (control). (For interpretation of the references to colour/colour in this figure legend, the reader is referred to the Web version of this article.)

fabricated MVP was further enabled and was first demonstrated by preparing ice templates to include biomolecules of FGF-2 and L-ascorbic acid 2-phosphate (A2-P), which were chosen with acknowledging their enhanced functionality in proliferation [65,66] and retained stem cell stemness [66], respectively, and the same fabrication process and mechanism was performed to produce the proposed MVP coating with decorated FGF-2 and A2-P functionalization within the coating layer. Selected human adipose-derived stem cell (hADSC) cell lines to verify the enhanced proliferation activity of fabricated MVP coatings, an established method to compare cellular activity in terms of the cell growth number from Day 1 to Day 5 (the effectiveness of FGF-2 became detectable) [67] was used and analysed by LIVE/DEAD staining for the analysis of cell numbers. The results in Fig. 4b indicate images of populated hADSC numbers by comparing Day 1 and Day 5, and a statistically significant difference was confirmed for the enhancement of hADSC proliferation due to FGF-2 decoration of the MVP coating, where the number of cells at day 5/day 1 was shown to have increased by $311 \pm 35\%$. In addition, the synergistic enhancement towards adipogenic activity of the cultured hADSCs by the side-by-side accommodation of both FGF-2 and A2-P in the MVP coating were observed by Oil Red O staining in Fig. 4b, and significant staining intensity as well as a consistent statistical analysis showed upregulated adipogenesis of hADSCs on the synergistic MVP coating compared to the pure MVP coating without any modification by $234 \pm 26\%$. Furthermore, due to enhanced stemness, anti-inflammatory, and antiapoptotic properties by forming spheroids of multipotent mesenchymal stem cells [68,69], the formation of hADSC spheroids of interest was enabled for the fabrication process of MVP, with a second and versatile combination including FGF-2 and chitosan molecules, which has been shown to influence the formation of spheroids spontaneously [70]. As seen in Fig. 4c, staining images showed an increased size and number of hADSC spheroids on the FGF-2/chitosan-modified MVP coatings, and the upregulated expression of stem cell pluripotent markers, including Oct4, Sox2, and nanog, also statistically confirmed the enhancement of hADSC spheroids on the proposed MVP coatings by $302 \pm 37\%$. Detailed data analysis of these self-renewal markers are included in the Supporting Information in Fig. S4. However, direct guidance of differentiation towards osteogenesis was further realized with the same concept by culturing hADSCs on a BMP-2-decorated MVP coating, and confirmation by immunofluorescence assay for OCN (osteocalcin) expression was measured at Day 21 to quantify the osteogenic differentiation activities of the cultured hADSCs on such MVP coatings. The recorded staining images and the statistical results in Fig. 4d unambiguously revealed enhanced osteogenic differentiation of hADSCs towards osteoblasts by BMP-2 functionality for the proposed modified MVP coatings by $43.3 \pm 14.7\%$. The versatility of exploiting the MVP coating was further extended to a more delicate differentiation manipulation system for odontogenesis, and a combination of culturing a sensitive cell line of human dental pulp stem cells (hDPSCs) and accommodating a functional substance of 45S5 Bioglass® in the MVP coating layer was performed. Confirmation of guiding hDPSCs towards odontogenesis by the modified MVP coating was conducted by observing the unique cellular morphology as well as the expression of osteocalcin in Fig. 4d, and the statistically consistent upregulation was also verified compared to the control groups, and an increase of $227 \pm 30\%$ was observed. In comparison to tissue culture plates, our previous reports have shown that the porous structures fabricated through vapour deposition and sublimation process have also showed better results in terms of cell adhesion and differentiation, thus increasing its potential applicability as coatings for tissue engineering [71,72].

In the fabrication of such a cell-laden MVP coating, the accommodation of living hADSCs was enabled by the aforementioned oil-in-water system in the ice template, where the cells were mixed well with oil and vascular endothelial growth factor (VEGF) was decorated in the same ice

template, before being inserted to the vapour deposition chamber to prepare a state-of-the-art MVP coating as that comprised living hADSCs and biofunctional VEGF constructs side-by-side, as depicted in Fig. 4e. As indicated in Fig. 4f, analysis by using SEM and LIVE/DEAD kit showed promised accommodations of hADSCs in the MVP coating layers that a spread cell morphology (SEM images), and a high survival rate of hADSCs was observed in the 2D and 3D fluorescence micrographs. In addition, the growth and proliferation activities were confirmed with increasing cell population from day 1 to day 4, and these analysis data are also included in the Supporting Information in Fig. S5. Such a sophisticated MVP coating was subsequently used for the culture of human umbilical vein endothelial cells (HUVECs). Based on acknowledging that hASDCs interacted as feeder cells with the growth activity of HUVECs during the maturation of HUVECs [73,74] and VEGF promotes angiogenesis inducing confluent microvascular endothelial cells forming capillary-like structures [75], the hypothesis is that the hADSCs/VEGF modified MVP coating provides an interface platform for the same enhancement and promotion of HUVEC growth and maturation activity, with the 3D images included in Supporting Information in Fig. S6. The coculture results in Fig. 4g at day 10 indicate that the nuclei of hADSCs were stained in the blue channel, while the CD 31 markers of HUVECs were stained in the green channel, and the proposed development of endothelial luminal networks was identified compared to a relatively supressed development of the HUVECs network for the control samples (pure MVP coatings without modifications). Quantification analysis of the measured tubular network length showed significance with aligned agreement with the staining results with an increase of $253 \pm 41.7\%$.

3. Conclusions

Coating technologies rely on mostly solution-based approaches and suffer limitations in providing simple functions but with complex procedures. Prospective coatings with multiple physical and chemical functionalities and simple fabrication methods require development. The vapour construction of MVP coatings introduced herein provides physical properties including varying pore size, mechanical strength, surface hydrophobicity, control elasticity in 2D and 3D, microstructuring, and compartmentalizing multiple functional additives with defined compositions and boundaries, i.e., spatial arrangement of distinct properties within one coating layer. Biochemically, the modified properties of MVP coatings, including enhanced biocompatibility and upregulation of stemness for stem cells, enhancement of stem cell proliferation, and important guidance of stem cells with defined differentiation pathways, were demonstrated by using the fabricated MVP coating surfaces for cell culture and coculture for adipogenesis, osteogenesis, odontogenesis, and angiogenesis. We foresee the applications of using the advanced coating technique and surface modifications for multiplying functions for prospective biomaterials to overcome upcoming challenges of more complex biotechnological applications.

Declaration of competing interest

The authors declare that they have no known competing financial interests or personal relationships that could have appeared to influence the work reported in this paper.

Acknowledgements

Appendix A. Supplementary data

Supplementary data to this article can be found online at https://doi.org/10.1016/j.mtbio.2022.100403.

References

[1] S.K. Nemani, et al., Adv. Mater. Interfac. 5 (24) (2018), 1801247.
[2] X. Liu, et al., J. Biomed. Mater. Res. 74A (1) (2005) 84.
[3] T. Kuila, et al., Prog. Mater. Sci. 57 (7) (2012) 1061.
[4] G. Wu, et al., J. Mater. Chem. B 3 (10) (2015) 2024.
[5] K.H. Ku, et al., Adv. Funct. Mater. 28 (42) (2018), 1802961.
[6] R. Shen, et al., Appl. Surf. Sci. 471 (2019) 43.
[7] X. Liu, S. Wang, Chem. Soc. Rev. 43 (8) (2014) 2385.
[8] E.E. Antoine, et al., Tissue Eng. B Rev. 20 (6) (2014) 683.
[9] B. Geiger, et al., Nat. Rev. Mol. Cell Biol. 10 (1) (2009) 21.
[10] M.J. Dalby, et al., Eur. J. Cell Biol. 83 (4) (2004) 159.
[11] M. Arnold, et al., Nano Lett. 8 (7) (2008) 2063.
[12] M. Arnold, et al., Soft Matter 5 (1) (2009) 72.
[13] Z. Nie, E. Kumacheva, Nat. Mater. 7 (4) (2008) 277.
[14] D. Falconnet, et al., Biomaterials 27 (16) (2006) 3044.
[15] B.D. Boyan, et al., Biomaterials 17 (2) (1996) 137.
[16] D. Falconnet, et al., Biomaterials 27 (16) (2006) 3044.
[17] M.J. Dalby, et al., Nat. Mater. 6 (12) (2007) 997.
[18] A.M. Ross, et al., Small 8 (3) (2012) 336.
[19] E.M. Sletten, C.R. Bertozzi, Angew. Chem. Int. Ed. 48 (38) (2009) 6974.
[20] A.J. Link, et al., J. Am. Chem. Soc. 126 (34) (2004), 10598.
[21] E. Saxon, et al., J. Am. Chem. Soc. 124 (50) (2002), 14893.
[22] K.E. Beatty, et al., J. Am. Chem. Soc. 127 (41) (2005), 14150.
[23] X. Li, et al., J. Am. Chem. Soc. 133 (29) (2011), 11147.
[24] M.M. Stevens, J.H. George, Science 310 (5751) (2005) 1135.
[25] J.H. Han, Chapter 9 - edible films and coatings: a review, in: J.H. Han (Ed.), Innovations in Food Packaging, second ed., Academic Press, San Diego, 2014, p. 213.
[26] M.M. Unterlass, Mater. Today 18 (5) (2015) 242.
[27] E. Avcu, et al., Prog. Mater. Sci. 103 (2019) 69.
[28] J. Martín, et al., Nat. Commun. 5 (2014) 5130.
[29] S.J. Bryant, et al., Biomaterials 28 (19) (2007) 2978.
[30] S.J. Hollister, Nat. Mater. 4 (7) (2005) 518.
[31] J.R. Tumbleston, et al., Science 347 (6228) (2015) 1349.
[32] R. Gauvin, et al., Biomaterials 33 (15) (2012) 3824.
[33] T. Subbiah, et al., J. Appl. Polym. Sci. 96 (2) (2005) 557.
[34] A. Moridi, et al., Surf. Eng. 30 (6) (2014) 369.
[35] F.T. Moutos, et al., Nat. Mater. 6 (2) (2007) 162.
[36] G.M. Gratson, et al., Nature 428 (6981) (2004) 386.
[37] Y. Kim, C.-J. Li, Green Synthesis and Catalysis 1 (1) (2020) 1.
[38] M.E. Alf, et al., Adv. Mater. 22 (18) (2010) 1993.
[39] H.-Y. Chen, Beilstein J. Nanotechnol. 8 (2017) 1366.
[40] J.B. Fortin, T.M. Lu, Chem. Mater. 14 (5) (2002) 1945.
[41] H.-Y. Tung, et al., Nat. Commun. 9 (1) (2018) 2564.
[42] H.-Y. Tung, et al., Appl. Mater. Today 7 (2017) 77.
[43] S. Deville, J. Mater. Res. 28 (17) (2013) 2202.
[44] G. John Morris, E. Acton, Cryobiology 66 (2) (2013) 85.
[45] T.-Y. Wu, et al., Coatings (12) (2020) 10.
[46] K.G. Libbrecht, Annu. Rev. Mater. Res. 47 (1) (2017) 271.
[47] N.D. Pawar, et al., J. Heat Tran. (6) (2019) 141.
[48] H.Y. Erbil, C.E. Cansoy, Langmuir 25 (24) (2009), 14135.
[49] G. McHale, et al., Langmuir 20 (23) (2004), 10146.
[50] D. Murakami, et al., Langmuir 30 (8) (2014) 2061.
[51] J.-T. Wu, et al., Chem. Mater. 27 (20) (2015) 7028.
[52] Y.-L. Lin, et al., Chem. Eng. Sci. 63 (1) (2008) 195.
[53] K.K. Liu, et al., J. Phys. Appl. Phys. 31 (3) (1998) 294.
[54] D.K. Owens, R.C. Wendt, J. Appl. Polym. Sci. 13 (8) (1969) 1741.
[55] R. Jafari, et al., Plasma Chem. Plasma Process. 33 (1) (2013) 177.
[56] M. Gazicki-Lipman, Shinku 50 (10) (2007) 601.
[57] C.C. Swan, I. Kosaka, Int. J. Numer. Methods Eng. 40 (16) (1997) 3033.
[58] G. Vozzi, et al., Biomaterials 24 (14) (2003) 2533.
[59] K. Adler, et al., Microsc. Res. Tech. 33 (3) (1996) 262.
[60] H. Zhang, A.I. Cooper, Adv. Mater. 19 (11) (2007) 1529.
[61] J. Kim, et al., Nat. Biotechnol. 33 (1) (2015) 64.
[62] Y.-R. Chiu, et al., Chem. Mater. 32 (3) (2020) 1120.
[63] B. Rubinsky, Heart Fail. Rev. 8 (3) (2003) 277.
[64] H. Feng, et al., Cryobiology 49 (3) (2004) 241.
[65] H.-J. Ahn, et al., FEBS (Fed. Eur. Biochem. Soc.) Lett. 583 (17) (2009) 2922.
[66] S.H. Bae, et al., Growth Factors 33 (2) (2015) 71.
[67] T.L. Riss, et al., Assay Guidance Manual [Internet, 2016.
[68] Y. Petrenko, et al., Stem Cell Res. Ther. 8 (1) (2017) 94.
[69] N.E. Ryu, et al., Cells 8 (12) (2019).
[70] N.-C. Cheng, et al., Biomaterials 33 (6) (2012) 1748.
[71] C.-W. Lin, et al., ACS Appl. Bio Mater. 3 (9) (2020) 5678.
[72] T.-Y. Wu, et al., Adv. Mater. Interfac. 8 (24) (2021), 2100929.
[73] A. Heidari-Moghadam, et al., Cell J 22 (Suppl 1) (2020) 19.
[74] Y.-M. Kook, et al., Nanomaterials 8 (2) (2018) 117.
[75] N. Ferrara, Arterioscler. Thromb. Vasc. Biol. 29 (6) (2009) 789.